Computational Investigation of Adaptive Deep Brain Stimulation

Christopher Y. Thang and Paul A. Meehan
School of Mechanical & Mining Engineering, The University of Queensland, Brisbane, Australia

Keywords: Closed-loop, Neural Feedback, Adaptive Deep Brain Stimulation, Parkinson's Disease.

Abstract: Deep Brain Stimulation of the sub-thalamic nucleus (STN) has been proven to be effective at reducing symptoms of patients with Parkinson's disease (PD). Currently an implanted pulse generator provides chronic electrical stimulation to the STN via an electrode and the stimulation parameters are chosen heuristically. Closed-loop Deep Brain Stimulation (DBS) has been proposed as an improvement to this, utilising neural signal feedback to select stimulation parameters, adjust the duration of stimulation and achieve better patient outcomes more efficiently. In this research, potential neural feedback signals were investigated using a computational simulation of the basal ganglia. It was found that the interspike-interval in the globus pallidus externus provided a possible metric for 'on' and 'off' states in Parkinson's disease. This parameter was subsequently implemented as neural feedback in an adaptive closed-loop DBS simulation and was shown to be effective. In particular, the thalamic relaying capability was evaluated using an Error Index (EI) and the adaptive DBS was found to reduce the EI to 2%, which compared with 20% for the PD case without DBS. This was achieved using 58% of the stimulation time used during continuous DBS, indicating a large reduction in DBS energy requirements. This selection and implementation of a potential neural feedback parameter will assist in developing improved implanted DBS pulse generators.

1 INTRODUCTION

Deep Brain Stimulation (DBS) has proven to be an effective method for relieving the symptoms of patients suffering from Parkinson's disease (PD), Essential Tremor (ET), dystonia (DT) and other neurological conditions. During the procedure, electrodes are inserted into targeted regions of the basal ganglia (Fig. 1) and connected to an Implanted Pulse Generator (IPG) positioned subcutaneously below the clavicle (Coyne, Silburn et al. 2006).

Currently the stimulation parameters for DBS are chosen heuristically, requiring periodic post-operative programming sessions to determine the optimum settings for symptom reduction for 6 months (Marjama-Lyons and Okun 2014). Neural plasticity effects, progression of the neurological disease, patient activity states and changes in the medication may all lead to changing stimulation requirements over time.

Closed-loop DBS has been proposed as an alternative to chronic open-loop DBS, utilising neural feedback signals to regulate the stimulation parameters. By sensing symptoms and activating stimulation when it is required, it is anticipated that the power consumption of the IPG may be reduced, symptom reduction may be improved and side-effects minimised. Figure 1 is a diagram of this closed-loop DBS concept with neural feedback being used to control the stimulation parameters.

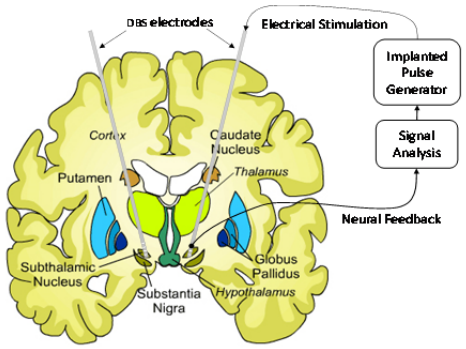

Figure 1: Diagram of closed-loop deep brain stimulation (Adapted from Huntington's Outreach Project for Education 2010).

Multiple research groups are currently investigating the feasibility of a system (Brain Institute, Utah; Neuromedical Control Systems Lab, John Hopkins University) and recently closed-loop DBS has been

Y. Thang C. and A. Meehan P..
Computational Investigation of Adaptive Deep Brain Stimulation.
DOI: 10.5220/0005212400660075
In *Proceedings of the International Conference on Bio-inspired Systems and Signal Processing* (BIOSIGNALS-2015), pages 66-75
ISBN: 978-989-758-069-7

trialled in patients (Little, FitzGerald et al. 2013). Prior to this, research has primarily been performed on primates or computational models. Carron et al. summarises the current closed-loop control approaches as delayed and multi-site stimulation; optimal control; proportional integral derivative control and adaptive stimulation (Carron, Chaillet et al. 2013). This work will focus on the latter control strategy.

A major challenge thus far has been determining a suitable neural feedback parameter that will characterise the severity of PD along with progression for the disease. Initial research has been conducted, testing the non-markovity spectrum as a neural measure however this work was focused on measuring linguistic response (Meehan, Bellette et al. 2011). It has previously been shown that Local Field Potential (LFP) recordings from the sub-thalamic nucleus (STN) show beta oscillations (8-35 Hz) in the PD state (Kühn, Kupsch et al. 2006, Kühn, Hariz et al. 2008). Recently, Little et al. went on further to successfully use this parameter as feedback in a clinical trial of adaptive DBS. Results showed a reduction in Unified Parkinson's Disease Rating Scale (UPDRS) motor scores by 27% in blinded assessment, when compared with continuous DBS (Little, FitzGerald et al. 2013). This new clinical research testing faces many difficulties and limitations that may be overcome with an efficient, validated computational model. Hence the present research aims to investigate and develop adaptive DBS in a computational environment to better understand the underlying neural mechanisms associated with this method of control.

This research focuses on the identification of an effective feedback parameter for closed-loop DBS and quantifying the feasibility of using the parameter in an adaptive DBS feedback system. A computational model of the basal ganglia based on the Rubin-Terman model (Rubin & Terman, 2004), is used to simulate DBS for PD in the STN (So, Kent et al. 2012). Neural output is then processed and feedback parameters for PD are investigated. In particular, the interspike interval is subsequently implemented as neural feedback in an adaptive closed-loop DBS simulation and its effectiveness quantified. It is expected that demonstrating the feasibility of closed-loop DBS for PD will provide a basis for future investigations into more efficient and effective systems for the treatment of PD and other neurological conditions.

2 METHODS

This research builds upon a well-developed model of the basal ganglia to develop an adaptive DBS simulation. The existing basal ganglia model is first presented, along with simulation parameters. This is followed by details of two signal analysis methods used to determine feedback parameters. A third signal analysis method is also presented which will be used to characterise the effectiveness of DBS.

2.1 Basal Ganglia Model

The basal ganglia (BG) is involved in the signal processing of a range of neural functions including voluntary motor movement, learning, cognition and emotion. In the BG, information is transmitted between nuclei via inhibitory and excitatory projections. Under the canonical model of BG motor loops, these projections form direct and indirect pathways through the BG. Figure 2 shows these pathways and synaptic connections on a cross-section of the BG.

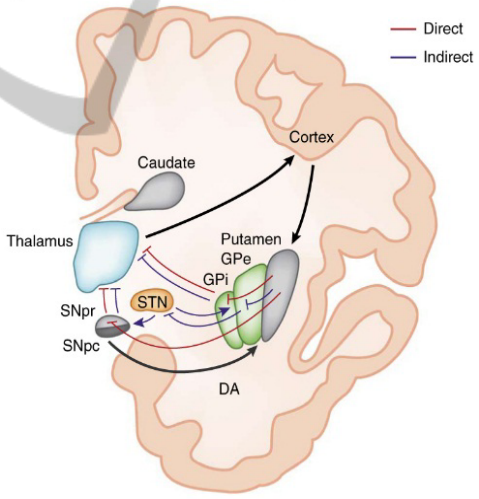

Figure 2: Diagram of the indirect (blue) and direct (red) pathways through the basal ganglia with excitatory and inhibitory connections represented with arrows and flat-ends respectively (Calabresi, Picconi et al. 2014).

In Figure 2, excitation of the **direct** pathway from the cortex has the effect of exciting the putamen, inhibiting the globus pallidus internus (GPi) and consequently disinhibition of the thalamus, resulting in ease of firing. Conversely, excitation of the **indirect** pathway from the cerebral cortex results in excitation of the putamen and consequently inhibition of the globus pallidus externus (GPe). This in turn leads to disinhibition of the sub-

thalamic nucleus (STN), excitation of the globus pallidus internus (GPi) and inhibition of the thalamus. When functioning correctly these competing pathways balance so that the thalamus operates correctly. A review of indirect/direct model suggests that it is still the most plausible BG model, although the possible role of pathway interactions must be revised in light of recent experimental work (Calabresi, Picconi et al. 2014).

An existing computational model of the BG, developed by So et al., was used to simulate neural output (So, Kent et al. 2012). This model is based on the Rubin-Terman model (Rubin and Terman, 2004) and it is a simplified model of the BG with components of the classical indirect and direct model. The excitatory and inhibitory synaptic connections of the computational BG model are summarised in Figure 3.

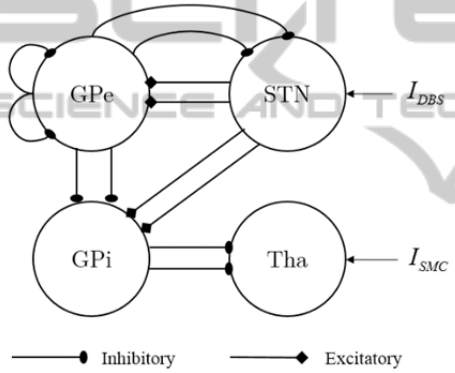

Figure 3: Excitatory and inhibitory synaptic connections used in the Basal Ganglia model.

In this model only the subcortical-thalamic region (Tha), subthalamic nucleus (STN), globus pallidus externus (GPe) and globus pallidus internus (GPi) are modelled. STN neurons are modelled with excitatory synapses to two GPe and GPi neurons; GPe neurons inhibit two STN, GPe and GPi neurons and each GPi neuron inhibits a Tha neuron. The DBS stimulation is applied to the STN and sensorimotor excitatory stimuli is inputted to the Tha.

The individual neuron membrane potentials were modelled using single-compartment conductance-based biophysical models of the form (Terman, Rubin et al. 2002, Rubin and Terman 2004),

$$C_m \frac{dV_\beta}{dt} = -I_L - I_{Na} - I_K - I_T - I_{Ca} - I_{ahp} - I_{\alpha-\beta} + I_{in}. \quad (1)$$

In (1), C_m is the membrane capacitance; V_β is the membrane potential; I_L, I_{Na}, I_K, I_T, I_{Ca} and I_{ahp} are the leak, sodium, potassium, low-threshold calcium, calcium and afterhyperpolarization currents respectively. Like most conductance based models, each of these currents is controlled via a time variant channel activation equation. Depending on the nuclei, the total cell current is a combination of these along with any current inputs, I_{in} which may include DBS, constant bias currents and sensorimotor input. The complete equations and model parameters used in this model are available in So et al. Synaptic currents $I_{\alpha-\beta}$ between neurons are represented as follows where α is a pre-synaptic and β is a post-synaptic neuron:

$$I_{\alpha\to\beta} = g_{\alpha\to\beta}\left[V_\alpha - E_{\alpha\to\beta}\right]\sum_j S_\alpha^j. \quad (2)$$

In (2), $g_{\alpha\to\beta}$ is the maximal synaptic conductance and $E_{\alpha-\beta}$ is the synaptic reversal potential. The gating of neurotransmitter receptors, S, varies from 0 to 1 and are described using an average response model. For STN and GPi efferents, a second order alpha synapse was used, where u(t) = 1 if the pre-synaptic cell spikes and is otherwise 0:

$$\begin{aligned} \frac{dS}{dt} &= z \\ \frac{dz}{dt} &= 0.234u(t) - 0.4z - 0.04S. \end{aligned} \quad (3)$$

The remaining connections were modelled using first order alpha synapses of the form:

$$\begin{aligned} \frac{dS}{dt} &= 2(1-S)H_\infty(V-20) - 0.04S \\ H_\infty(v) &= 1/\left[1+\exp\left(\frac{-v+57}{2}\right)\right]. \end{aligned} \quad (4)$$

In the Parkinson's disease state, the loss of dopamine results in disinhibition of the GPi via the direct pathway and increased inhibition of the GPe, disinhibition of the STN and further increased activity of the GPi via the indirect pathway. PD states were simulated using a reduction in applied currents to the STN, GPe and GPi as summarised in Table 1 (So, Kent et al. 2012).

Table 1: Applied currents in PD and Healthy states.

Neural State	$I_{app-STN}$	$I_{app-GPe}$	$I_{app-GPi}$
Healthy	33 μA/cm^2	20 μA/cm^2	21 μA/cm
Parkinson's	23 μA/cm^2	7 μA/cm^2	15 μA/cm^2

This produced firing behaviour consistent with humans, rodents and primates with PD (So, Kent et al. 2012). The reduction in the GPe applied current is the largest which corresponds with disinhibiting the GPi and STN.

High-frequency DBS input into the STN was modelled using the Heavyside step function, H,

$$I_{DBS} = i_{DBS}H(\sin(2\pi f_{DBS}\,t)) \times \left[1 - H(\sin(2\pi f_{DBS}(t+\delta_{DBS})))\right], \quad (5)$$

where i_{DBS} is the stimulation amplitude, f_{DBS} is the stimulation frequency and δ_{DBS} is the pulse width. Simulations were run in MATLAB (MATLAB 8.3, The MathWorks Inc., Natick, MA, 2014). The simulated time was 6000 ms, with 30 neurons per nuclei, 130 Hz stimulation and a time-step of 0.01 ms using Euler's forward difference method unless otherwise indicated.

2.2 Signal Analysis

The interspike interval and synchrony measures are presented in this section and will be applied to the spike-trains from the BG model. The third measure, Error Index, tests for relaying fidelity and will be used to examine DBS effectiveness.

2.2.1 Interspike Interval

The Interspike Interval (*ISI*) is defined as the time between subsequent action potentials of the spike train. The mean ISI of a neuron is often calculated to be,

$$\overline{ISI} = \frac{1}{n}\sum_{i=1}^{n} ISI_i, \quad (6)$$

where n is the number of spikes and ISI_i is the interval between two spikes. Whilst regularly used for leaky integrate and fire (LIF) models, it requires individual spike train data for neurons. This is suitable for computational models but difficult to obtain from in-vitro microelectrode recordings (MER), unless a single-unit MER is used. The threshold for peak detection was set at -10 mV and the average and standard deviation of the ISI was then taken across all 30 neurons, for each nuclei. This resulted in a dataset of approximately 2,000 spikes for the thalamic region to 14,000 spikes for the GPi.

2.2.2 Synchrony

It has been proposed that in PD states, increased synchrony occurs in the GPi and that synchrony is reduced in the thalamic region (Rubin and Terman 2004). Golomb proposes the following measure for neuronal synchrony χ (Golomb and Rinzel 1993):

$$\chi^2(N) = \frac{\sigma_V^2}{\frac{1}{N}\sum_{i=1}^{N}\sigma_{V_i}^2}. \quad (7)$$

In (7) the variance of the total voltage is defined as,

$$\sigma_V^2 = \left\langle V(t)^2 \right\rangle_t - \left[\left\langle V(t)\right\rangle_t\right]^2,$$
$$\text{where } \left\langle ... \right\rangle_t = \frac{1}{T_m}\int_0^{T_m} dt \text{ and } V(t) = \frac{1}{N}\sum_{i=1}^{N} V_i(t). \quad (8)$$

Similarly the variance of individual neurons is defined as:

$$\sigma_{V_i}^2 = \left\langle V_i(t)^2 \right\rangle_t - \left[\left\langle V_i(t)\right\rangle_t\right]^2. \quad (9)$$

It can be seen that the neuronal synchrony measure relies on voltage data from a population of neurons which is only readily obtained from computational models. For completely asynchronous behaviour, it is expected that the synchrony measure will decrease as the number of neurons sampled is increased. Otherwise, for synchronous and weakly synchronised neurons, the degree of synchrony will be constant for varying N.

2.2.3 Error Index

Rubin and Terman have proposed an Error Index (EI) to characterise the relaying fidelity of the thalamic region (Rubin and Terman 2004). The EI is determined as,

$$EI = \frac{1}{n}\left(\sum E_{misses} + \sum E_{false}\right), \quad (10)$$

where n is the number of input stimuli, E is an error from either a false positive or a miss. False positives are defined as spikes occurring without stimulus and multiple spikes in response to a single stimulus. Misses are defined as a failure to respond within 10 ms of a stimulus. High EI values correspond with poor thalamic relaying capability of sensorimotor input. In this testing, the EI is evaluated over a sample size of approximately 800 input stimuli. This EI will be used to characterise the effectiveness of adaptive DBS in maintaining relaying capacity in the thalamic region of sensorimotor input and compared with results for healthy, PD and continuous DBS states.

3 RESULTS

In this section the signal analysis results are used to determine an optimum neural feedback parameter. After being selected, the parameter is then used as neural feedback in an adaptive DBS simulation. The effectiveness of the adaptive DBS is compared with healthy, PD and continuous DBS states, using the Error Index measure to test for thalamic fidelity.

3.1 Signal Analysis

Two signal analysis methods are presented here as possible feedback parameters. The results from the interspike interval analysis is shown first, followed by Golomb's synchrony measure.

3.1.1 Interspike Interval

The Interspike Interval (ISI) results have been plotted in Figure 4 for each of the nuclei in the healthy, PD and PD with DBS states. When in the PD state an increase in ISI can be observed in the thalamic region due to misfiring. In the STN, the ISI is reduced when DBS is applied since the neurons are triggered to fire in unison at the 130 Hz stimulation frequency. The GPi has a reduced ISI when DBS is applied and the ISI in the GPe increases for the PD state.

All four nuclei have an increase in ISI variance (square of the standard deviation) for the PD states. In particular, the standard deviation of GPe ISI increases the most, rising by 380% in the PD state (see error bars in Figure 4). This compares with a corresponding 87% increase in ISI. This increase in variance can be attributed to periodic periods of spiking in the GPe instead of sustained firing. Once DBS is applied, GPe ISI and standard deviation of ISI return to similar values to the healthy state. ISI variance in the thalamic region also exhibits similar increases. This could be explained through BG loops (Figure 3) as reduced activity in the GPe resulting in disinhibition of the GPi and consequently increased inhibition of the thalamus. This significant variation in variance in the GPe shows potential as a possible neural feedback parameter for 'on' and 'off' PD states.

The response of the ISI was then tested for the four nuclei when the DBS frequency is adjusted. This was performed to determine if there were any relationships between DBS frequency and ISI measures. A batch script was run increasing the frequency incrementally in intervals of 1 Hz from 0 to 120 Hz. The STN mean ISI was found to be inversely proportional to frequency, as the STN neurons are triggered to fire by the DBS.

In Figure 5, high fluctuating values are observed in the ISI variance for thalamic neurons when stimulation frequency is less than 52 Hz and consistent low values are observed above 70 Hz. From the results in Figure 4, it is assumed that low variance corresponds with the DBS working effectively and returning the BG to a healthy state. In Figure 5, a spike in ISI and ISI variance occurs at 40-50 Hz suggesting that 40-50 Hz DBS may be counter-effective. Similar trends were observed in the GP region with stimulation appearing to be ineffective for frequencies lower than 50 Hz. This is consistent with the current understanding that low-frequency DBS (<50 Hz) can be counter-effective although the neural mechanisms for this are still unknown (McConnell, So et al. 2012).

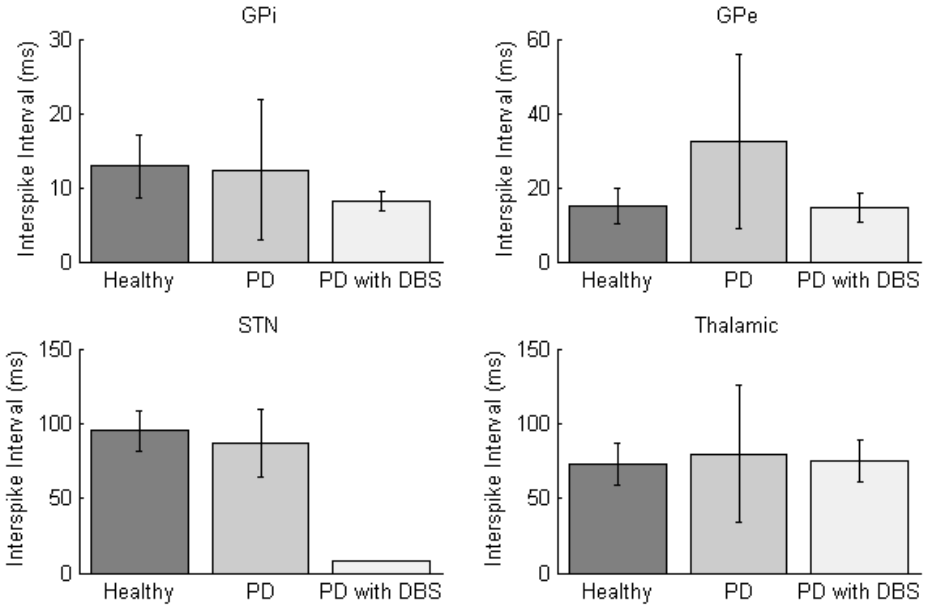

Figure 4: Mean Interspike Interval plotted for each of the four nuclei at healthy, Parkinson's disease and DBS corrected states with the standard deviation represented as error bars. Stimulation parameters are set at 130 Hz with pulse width of 0.6 ms and amplitude of 350 $\mu A/cm^2$.

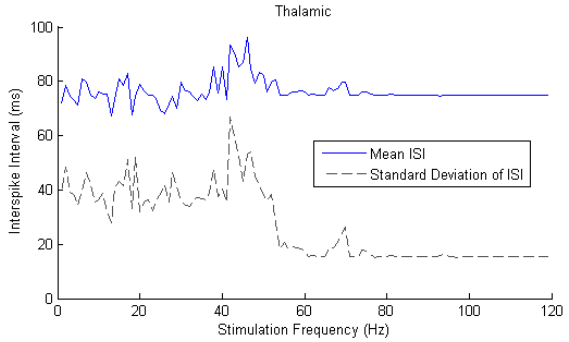

Figure 5: Thalamic ISI for varying DBS frequency.

The ineffectiveness of low-frequency DBS (<50 Hz) and consistent effect at high frequencies (>80 Hz) suggests that DBS frequency would not be an effective stimulation control parameter.

3.1.2 Synchrony

The synchrony of the four nuclei in the healthy, PD and PD with 130 Hz DBS states can be seen in Figure 6. The measure has been plotted as a function of N, the number of neurons included in the measure. For completely asynchronous systems, it is expected that the synchrony measure will go to zero as N approaches large values. Clearly in this case this testing is limited since only 30 neurons were used in each nuclei.

Monotonic decreasing trends towards zero should be observed if the system is asynchronous and here it can be seen that the four nuclei are each not completely asynchronous. The thalamic nuclei has a 37% reduction in synchrony for the PD state due to misfiring and GPi inhibition. After DBS is applied, synchrony increases to value of 1, indicating that sensorimotor input is being transferred correctly. In all other regions, the DBS results in increased degrees of synchrony, with the greatest increase occurring in the STN where the DBS is applied.

It appears that synchrony in the thalamic region could be used as a feedback signal for the PD state, although the DBS state appears to lead to a higher degree of synchrony than the healthy state. It should also be noted that this measure requires the individual membrane potential data of a large number of neurons, which is only obtainable in computer simulations at this stage.

3.2 Adaptive DBS

An adaptive DBS scheme was implemented utilising ISI variance in the GPe as a trigger for stimulation. The motivation for this selection was based on the largest rise between PD and healthy states. The adaptive DBS stimulation threshold was set for a GPe ISI standard deviation greater than 13 ms based on data from the preceding 500 ms. This threshold was chosen to be slightly above the variance of the healthy state. A block diagram of this adaptive DBS system is shown in Figure 7.

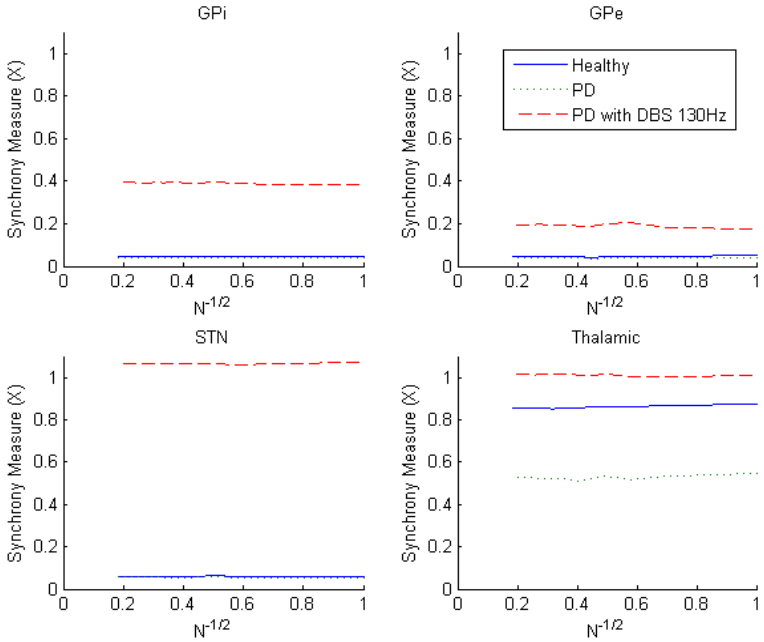

Figure 6: Synchrony for the four nuclei plotted as a function of the number of neurons included in the measure.

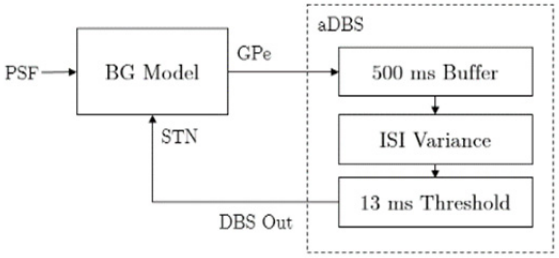

Figure 7: Block diagram of the adaptive DBS system.

Dynamic Parkinson's disease conditions were created by applying a stepped PD severity input. A Parkinson's Severity Factor (PSF) on a scale of 0-1 is used to adjust the PD severity and the applied current in the STN, GPe and GPi was modified as follows:

$$I_{app-PD} = I_{base} - PSF \times I_{PD}. \quad (11)$$

The base current values I_{base} in (11) were the healthy applied currents and I_{PD} was determined as the difference between healthy and Parkinsonian states in Table 1. Once stimulation is triggered, the aDBS remains on for at least 150 ms before switching off.

The resulting spike trains in the basal ganglia can be seen in Figure 8 for PD, with adaptive DBS using GPe ISI variance as a feedback parameter to respond to stepped PD severity input. For convenience, a close-up of 1000-3000 ms is shown in Figure 9 so that the effects of adaptive DBS may be compared with the PD state. In Figure 8 [A], between 0 and 2000 ms, the BG is in the PD state. By comparing the neuron spike train (above) with the sensorimotor input (below), errors in the thalamic relaying capability can be observed. These errors are highlighted in Figure 9 [A], with two misfires observed between 1000-2000 ms. At the same time PD conditions are evident in Figure 8 [C] & [D] with bursting firing behaviour in the GPe and GPi. This is firing behaviour is seen clearly in Figure 9 [C] & [D], (left) with varying intervals between bursts.

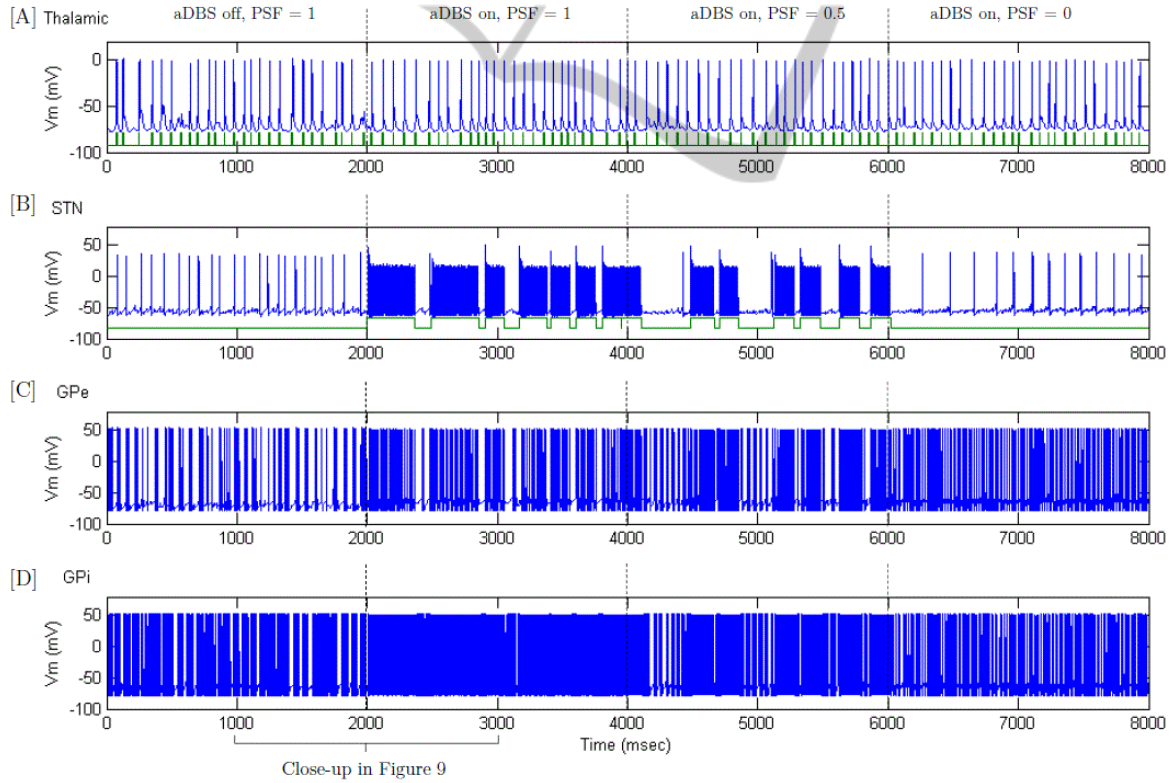

Figure 8: Adaptive DBS (aDBS) using variance of ISI from the GPe as a feedback signal. Between 0-2000 ms the Parkinson's severity is at a maximum and aDBS is not turned on; at 2000 ms the aDBS is initiated; between 4000-6000 ms Parkinson's severity is stepped down to 50% and at 6000 ms the severity is further reduced to 0%. [A] Spike-train from a thalamic neuron (above) with sensorimotor input (below); [B] Spike-train from a sub-thalamic nucleus neuron (above) with DBS stimulation times (below); [C] Spike-train from a globus pallidus externus neuron and [D] Spike-train from a globus pallidus internus neuron.

When adaptive DBS (aDBS) is initiated at 2000 ms, the STN stimulation triggers periodically to maintain consistent firing in the GPe as seen in Figure 8, [B]. Figure 9 shows a close-up of this transition for thalamic, STN, GPe and GPi neurons. It can be seen in Figure 9 [B], (right) that the application of stimulation to the STN triggers high-frequency STN firing and restores thalamic throughput capability in Figure 9 [A], (right). The short periods where the aDBS switches off stimulation does not appear to lead to errors in the thalamic relaying of sensorimotor input.

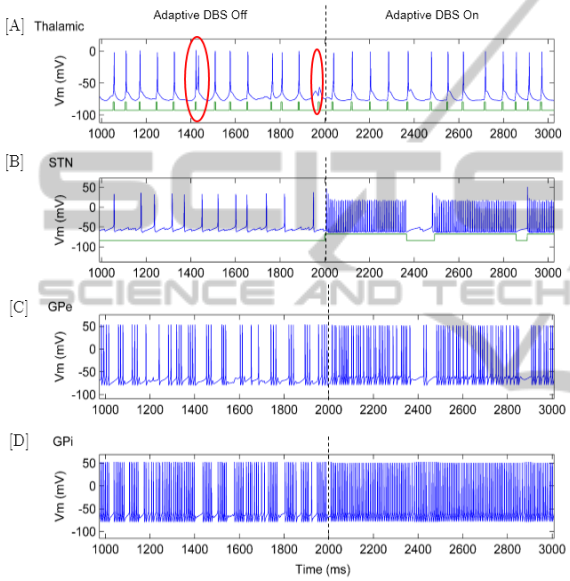

Figure 9: The transition from adaptive DBS being 'off' to 'on' for an [A] thalamic, [B] sub-thalamic nucleus, [C] globus pallidus externus and [D] globus pallidus internus neuron; misfires in the thalamic region are circled in red.

In Figure 9 [C], when aDBS control is initiated the GPe firing rate is steady during periods when stimulation is on. Once the standard deviation of the GPe ISI is reduced below the threshold, the stimulation switches off and the GPe returns to bursting behaviour (e.g. 2370-2460 ms). If the standard deviation of the GPe ISI exceeds the threshold, stimulation is turned on again and this 'on' and 'off' cycle can be seen in Figure 8 [B] until the Parkinson's severity is lowered. The GPi does not appear to be affected by the short periods where the stimulation is switched off which suggests a delayed response. The continuous firing of the GPi during these short periods of no stimulation may be an important factor in the success of the aDBS in maintaining reliable thalamic throughput.

During 4000-6000 ms in Figure 8, the severity of Parkinson's is reduced to 50% and a reduction in GPe bursting behaviour is observed in [C] due to the increase in applied current. As a result, the period between STN stimulation triggering in [B] increases since there is less variance in the GPe ISI. This reduction in stimulation 'on' time does not appear to impact the thalamic relaying capability. Finally, when healthy conditions are imposed from 6000 ms, regular GPe firing is observed in Figure 8 [C] and consequently the aDBS control scheme no longer triggers stimulation. No bursting is observed in the GPe or GPi and the thalamic neuron transmits the sensorimotor input correctly.

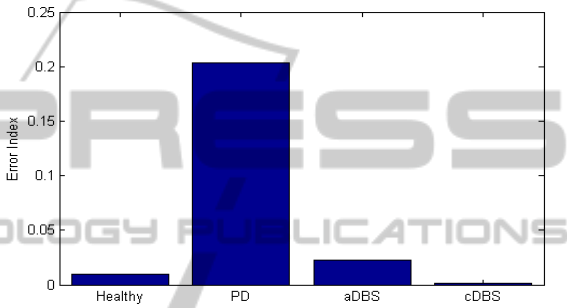

Figure 10: Error Index results for healthy, Parkinson's disease (PD), PD with adaptive DBS and PD with continuous DBS states.

The Error Index (EI) is used to determine the change in thalamic relaying capability when adaptive DBS and continuous DBS are applied. These results are compared to healthy and PD states in Figure 10 for a stepped PSF input identical to Figure 11, [A].

Figure 10 shows that adaptive DBS was successful in reducing the EI from 20% to 2%. The healthy state had an error index of 1% and the PD with cDBS state had an EI of 0.2%. Although the aDBS did not reduce the EI to the levels of cDBS, occasional misfiring does occur in the healthy state and this is most likely an acceptable result. The clear advantage of aDBS here is that only 58% of stimulation was used in comparison with the cDBS system whilst achieving a 95% of the reduction towards the healthy state. If further tuning of the aDBS is performed along with the implementation of more advanced control methods, it is possible that healthy conditions could be achieved with substantial power savings.

The effectiveness of adaptive DBS was further quantified by investigating the change in the GPe ISI standard deviation with respect to Parkinson's Severity Factor, as shown in Figure 10. A stepped PSF input has been inputted to the simulation with

and without aDBS applied. When no DBS is applied the standard deviation of the GPe ISI remains well above the healthy threshold values for a maximum PSF. It can be noted that the variance has a delayed response to a stepped reduction to the PSF at 2000 ms. When aDBS is operating, the standard deviation reaches the threshold regularly and triggers STN stimulation. Comparing Figure 11 [C] and [D] to [B] it is deduced that aDBS is effective in maintaining healthy levels of variance in the GPe spike train.

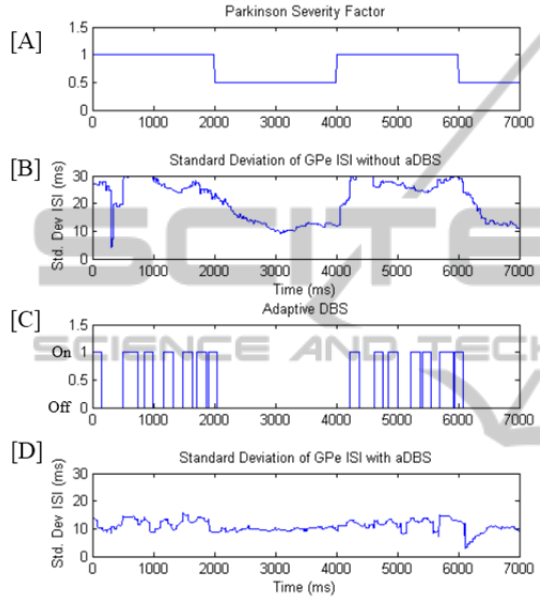

Figure 11: [A] Stepped inputs of Parkinson's Severity Factor over time; [B] Standard deviation of GPe ISI without aDBS being applied; [C] & [D] Adaptive DBS with stimulation time (top) and corresponding Std. Dev of GPe ISI (bottom).

4 CONCLUSIONS

In this investigation we examined the feasibility of interspike interval (ISI) and synchrony as feedback parameters for closed-loop DBS. Between the healthy, Parkinson's Disease (PD) and PD with DBS states, an 87% increase in interspike interval was observed in the globus pallidus externus (GPe). It is hypothesised that this increase in interval between spikes results in disinhibition of the globus pallidus internus (GPi) which in turn inhibits the thalamus and prevents the thalamus from relaying sensorimotor input effectively. Underlying rhythmicity in the GPi appears to further inhibit the thalamus. In the PD state, the standard deviation of GPe ISI was found to increase by 380% from the healthy and PD with DBS states and thus demonstrated potential as a feedback parameter.

Synchrony in the thalamic region was found to drop by 37% from the healthy to PD state. It should be noted that once DBS was initiated, the synchrony measure in the thalamic region exceeded the healthy levels. Other regions of the basal ganglia only exhibited synchrony changes for the PD with DBS state. Due to the practical difficulties associated with obtaining multiple neuron recordings in a clinical setting for the synchrony measure, the standard deviation of ISI in the GPe was thus investigated further in a closed-loop DBS simulation.

An adaptive DBS (aDBS) closed-loop control scheme was used, where stimulation was turned on or off depending on whether the GPe ISI Std. Dev exceeded a threshold of 13 ms. The response of the system was tested for stepped inputs for varying Parkinson's Severity Factors (PSF). The aDBS scheme was successful in improving the thalamic relaying capability, with an Error Index (EI) of 2%. This compared with 1% for the healthy state and 20% for PD with no DBS. In this implementation, the aDBS applied stimulation for 58% of the total time during a stepped PSF input, indicating a substantial reduction in DBS power consumption.

Challenges still remain between testing in the computational environment and implanting this technology in patients. Although clinical trials have already successfully been performed by Little et al. using beta-oscillations as a feedback parameter, those trials were performed using a wired connection between dedicated signal processing tools, laptop and patient. The miniaturisation of these systems into an IPG has yet to be achieved and this work faces similar challenges with the signal analysis tools. The accuracy of ISI interval sampling has also not been tested in patients for this work although single-cell microelectrode recordings may offer one potential solution towards gathering the spike interval data.

In this computational simulation, variance (square of the standard deviation) in interspike interval of the globus pallidus externus has successfully been used as a feedback parameter for aDBS. Research into more advanced control methods such as Proportional-Integral control of stimulation amplitude may offer further opportunities to improve stimulation efficiency. These alternate control methods will require tuning to overcome the highly non-linear 'all-or-none' firing dynamic of neurons. Despite the widespread use of such controllers in other applications, it is possible that adaptive DBS may achieve a profile

closer to the healthy state, due to the 'all-or-none' nature of the control method.

ACKNOWLEDGEMENTS

The authors would like to acknowledge Professor Peter Silburn (Asia-Pacific Centre for Neuromodulation) for his expertise in clinical aspects of this research along with Professor Tipu Aziz (Oxford Functional Neurosurgery) for his research guidance.

REFERENCES

Calabresi, P., B. Picconi, A. Tozzi, V. Ghiglieri and M. Di Filippo (2014). "Direct and indirect pathways of basal ganglia: a critical reappraisal." Nat Neurosci 17(8): 1022-1030.

Carron, R., A. Chaillet, A. Filipchuk, W. Pasillas-Lépine and C. Hammond (2013). "Closing the loop of deep brain stimulation." Frontiers in Systems Neuroscience 7: 112.

Coyne, T., P. Silburn, R. Cook, P. Silberstein, G. Mellick, F. Sinclair, G. Fracchia, D. Wasson and P. Stanwell (2006). "Rapid subthalamic nucleus deep brain stimulation lead placement utilising CT/MRI fusion, microelectrode recording and test stimulation." Acta Neurochirurgica Supplement 99: 49-50.

Golomb, D. and J. Rinzel (1993). "Dynamics of globally coupled inhibitory neurons with heterogeneity." Physical Review E 48(6): 4810-4814.

Huntington's Outreach Project for Education, S. U. (2010). "HOPES Brain Tutorial - Basal Ganglia." Retrieved 14 November, 2014, from http://hopes .stanford.edu/sites/hopes/files/f_ab18bslgang.gif.

Kühn, A. A., M. I. Hariz, W. Vandenberghe, B. Nuttin, P. Brown, F. Kempf, C. Brücke, L. Gaynor Doyle, I. Martinez-Torres, A. Pogosyan, T. Trottenberg, A. Kupsch, G.-H. Schneider, Neurokirurgi, f. Medicinsk, n. Farmakologi och klinisk and u. Umeå (2008). "High-frequency stimulation of the subthalamic nucleus suppresses oscillatory beta activity in patients with Parkinson's disease in parallel with improvement in motor performance." The Journal of Neuroscience 28(24): 6165-6173.

Kühn, A. A., A. Kupsch, G. H. Schneider and P. Brown (2006). "Reduction in subthalamic 8–35 Hz oscillatory activity correlates with clinical improvement in Parkinson's disease." European Journal of Neuroscience 23(7): 1956-1960.

Little, S., J. FitzGerald, A. L. Green, T. Z. Aziz, P. Brown, A. Pogosyan, S. Neal, B. Zavala, L. Zrinzo, M. Hariz, T. Foltynie, P. Limousin and K. Ashkan (2013). "Adaptive deep brain stimulation in advanced Parkinson disease." Annals of Neurology 74(3): 449-457.

Marjama-Lyons, J. and M. Okun (2014). Parkinson's Disease: Guide to Deep Brain Stimulation Therapy, National Parkinson Foundation.

McConnell, G. C., R. Q. So, J. D. Hilliard, P. Lopomo and W. M. Grill (2012). "Effective deep brain stimulation suppresses low-frequency network oscillations in the basal ganglia by regularizing neural firing patterns." The Journal of neuroscience : the official journal of the Society for Neuroscience 32(45): 15657-15668.

Meehan, P. A., P. A. Bellette, A. P. Bradley, J. E. Castner, H. J. Chenery, D. A. Copland, J. D. Varghese, T. Coyne and P. A. Silburn (2011). Investigation of the non-markovity spectrum as a cognitive processing measure of deep brain microelectrode recordings. Biosignals 2011. Rome, Italy, SciTePress: 144-150.

Rubin, J. E. and D. Terman (2004). "High frequency stimulation of the subthalamic nucleus eliminates pathological thalamic rhythmicity in a computational model." Journal of Computational Neuroscience 16(3): 211-235.

So, R. Q., A. R. Kent and W. M. Grill (2012). "Relative contributions of local cell and passing fiber activation and silencing to changes in thalamic fidelity during deep brain stimulation and lesioning: a computational modeling study." Journal of Computational Neuroscience 32(3): 499-519.

Terman, D., J. E. Rubin, A. C. Yew and C. J. Wilson (2002). "Activity patterns in a model for the subthalamopallidal network of the basal ganglia." The Journal of Neuroscience 22(7): 2963-2976.